Signature of Atomic Structure in the Quantum Conductance of Gold Nanowires

Varlei Rodrigues,[1,2] Tobias Fuhrer,[1] and Daniel Ugarte[1,*]

[1]*Laboratório Nacional de Luz Síncrotron, C.P. 6192, 13083-970 Campinas SP, Brazil*
[2]*Instituto de Física "Gleb Wataghin," UNICAMP, C.P. 6165, 13083-970 Campinas SP, Brazil*

(Received 14 April 2000)

We have used high resolution transmission electron microscopy to determine the structure of gold nanowires generated by mechanical stretching. Just before rupture, the contacts adopt only three possible atomic configurations, whose occurrence probabilities and quantized conductance were subsequently estimated. These predictions have shown a remarkable agreement with conductance measurements from a break junction operating in ultrahigh vacuum, corroborating the derived correlation between nanowire atomic structure and conductance behavior.

PACS numbers: 68.65.+g, 61.16.Bg, 73.50.–h

Metallic nanowires (NW) display interesting quantum phenomena that may be exploited to generate novel electronic devices. NWs can be easily generated by putting in contact two surfaces which are subsequently pulled apart. During the NW elongation, the conductance displays flat plateaus and abrupt jumps, which take a value of approximately a conductance quanta $G_0 = 2e^2/h$ (where e is the electron charge and h is Planck's constant) [1].

Several approaches have been used to study the conductance of metal NWs, showing conductance curves having plateaus and jumps, but displaying different profiles [2–7]. Thus, statistical methods are applied to analyze the average behavior [8,9], hindering a detailed study of NW transport properties [3]. Rubio *et al.* [5] have shown that abrupt conductance jumps are associated with a mechanical force relaxation; this has been attributed to atomic rearrangements whose nature is not yet fully understood, although many molecular dynamic simulations have been undertaken [2,4,8–13].

Recently, Onishi *et al.* [14] have used a simplified scanning tunneling microscope (STM) to generate gold NWs *in situ* in a high resolution transmission electron microscopy (HRTEM) while simultaneously recording the conductance. These studies revealed the existence of suspended gold atom chains whose conductance was $\sim 1G_0$ [14,15]. However, using a STM-based TEM sample holder [14,16], it will certainly be very difficult and time consuming to get a representative sampling of all possible NW structures. A major difficulty is the NW lifetime, which must be compatible with the HRTEM image acquisition requirements: (a) ~ 0.5–1.0 s for high quality micrographs, or (b) 0.033 s for individual video frames. In conductance experiments using dedicated STMs, a conductance curve lasts tens to hundreds of ms [17].

Only a weak relation has been established between structure evolution and the conductance curve profile. It would be worthwhile to understand the factors governing the conductance behaviors derived from a typical transport experiment [3,6,7,17], where a relevant physical aspect would be the structure of the touching surfaces, as well as their relative crystallographic orientation. These parameters cannot be controlled, and certainly they lead to the generation of a different NW atomic arrangement for each measurement; then the related conductance curve is not repetitive [2–4,6–9].

In this work, we have addressed the correlation between gold NW structure and the quantized conductance behavior. Using HRTEM, we have observed that just before rupture there are only three possible NW structures and, by means of simple crystallographic arguments, we have explained the adopted atomic arrangement and predicted their occurrence probability. Subsequently, we have estimated their conductance evolution; these predictions showed a remarkable agreement with transport measurements from a mechanically controllable break junction (MCBJ) [6,18] operating in ultrahigh vacuum (UHV).

We have generated NWs *in situ* in a HRTEM by focusing the electron beam (current density 120 A/cm^2) on different sites of a self-supported metal thin film (making holes and allowing them to grow [14,19]) until a nanometric neck was formed inside or between grains, and then reduced the electron beam intensity (30 A/cm^2) in order to perform the image acquisition. We have used a polycrystalline gold film (5 nm thick, average grain size 50–100 nm) in order to generate NW with different elongation directions or formed between grains with different orientations. An enhanced NW stability is obtained due to the monolithic structure of the system formed by the NW, the apexes, and the surrounding region of the metal film. Although the electron current is diminished, the NW apexes spontaneously show relative displacement/rotation inducing a slow elongation and thinning of the constriction between them. These movements are probably due to a thermal deformation of the whole thin film. This fact, as well as the long NW lifetime ($\sim$min), suggests that the electron beam does not induce important structural changes and that the NW evolution can be mainly attributed to strain. In addition, the intense electron irradiation is also helpful to clean the gold nanostructures, because it transforms an *a-C* contamination (if present) into spherical multishell fullerenes [20]. Our HRTEM observations were performed using

 0031-9007/00/85(19)/4124(4)$15.00

a JEM 3010 ARP (LME/Lab. Nac. Luz Síncrotron, Campinas, Brazil). All presented micrographs were acquired using a CCD camera (Gatan MSC 794, ~1 s acquisition time); also a TV camera (Gatan 622SC) was used for time resolved HRTEM recordings.

NW transport experiments were performed using a UHV-MCBJ [18] ($<10^{-10}$ mbar), where a $\phi = 75$ μm gold wire (99.99%) was broken *in situ* and subsequently NWs were generated from these clean surfaces. The electronic measurement system consists of a homemade voltage source and a current-voltage converter associated with an 8 bit digital oscilloscope (Tektronic TDS540C). The applied voltage was 100 mV, and the conductance was measured in the [0, 2.7] G_0 range with a relative error $(\Delta G/G) \sim 10^{-4}$.

The generation of NWs in the HRTEM is very efficient and the recording of atomic resolution images is possible due to their slow elongation and long lifetime (evolution from a few atoms thick neck to rupture takes 1–30 min). Figure 1 shows a series of snapshots of a complete elongation process of a NW along the [111] direction (henceforth noted [111] NW), where the neck shows the expected biconical structure [13,21].

The analysis of numerous HRTEM images (more than 300) pointed out that during the final stretching steps (a) gold NWs are crystalline and free of defects [22], and (b) three distinct NW structures are merely observed, because the atomic arrangement adjusts such that one of the [111]/[100]/[110] gold zone axes lies approximately parallel to the elongation direction, independent of the apex crystal orientation. This agrees with physical intuition of metal atom behavior, because these directions allow the highest gold atom packing at the constriction cross-section plane. The structural adjustment is mainly concentrated around the narrowest neck region, because there the energy cost would be lower. Figures 2(c)–2(e) display an example where the NW has initially a rod shape [[110] NW, Fig. 2(c)]. As the apexes are moving horizontally in opposite directions, they induce an out-of-axis NW elongation in such a way that the apex tip structure becomes oriented with a [111] axis close to the stretching direction [Fig. 2(e)]. This can be verified by a ~5° rotation (clockwise) of the upper apex (111) planes between Figs. 2(c) and 2(e).

In addition, using time resolved HRTEM, we have observed that NWs along the [111] and [100] directions show a ductile behavior, generating constrictions with bipyramidal shape [Fig. 1 and 2(a)] that gradually evolve to one-atom-thick constrictions [Figs. 2(a)–2(e)]. These contacts frequently adopt a chain structure (2–4 atoms long, bond distance ~0.36 nm) in agreement with previous UHV-TEM results [14]. In contrast, when the elongation is parallel to a [110] direction, NWs always display a rodlike morphology [16,19] with aspect ratios in the 3–10 range [Fig. 2(b)]. Also the rupture process is unlike, because time-resolved HRTEM has shown that thin [110] NWs seem to be brittle, breaking abruptly when they are still 3–4 atoms thick.

All the observed neck morphologies can be deduced by means of the geometrical Wulff construction, which has been extensively applied to predict gold nanoparticle faceting [23]. In these terms, it can be derived that

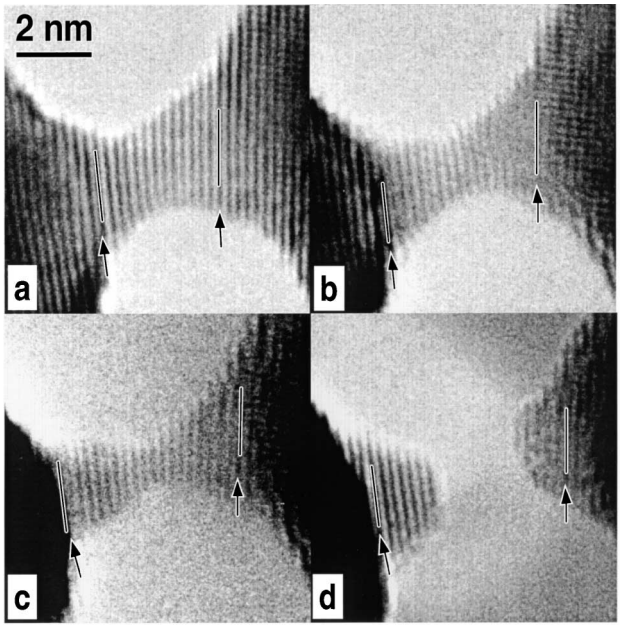

FIG. 1. (a)–(d) NW evolution when stretched along the [111] direction; atomic positions appear dark: 0, 120, 193, and 215 s. The neck is formed by ~12, 16, 18 planes from (a) to (c) (counted between two undeformed regions indicated by arrows). After the rupture (d), the two apexes reorganize and retract.

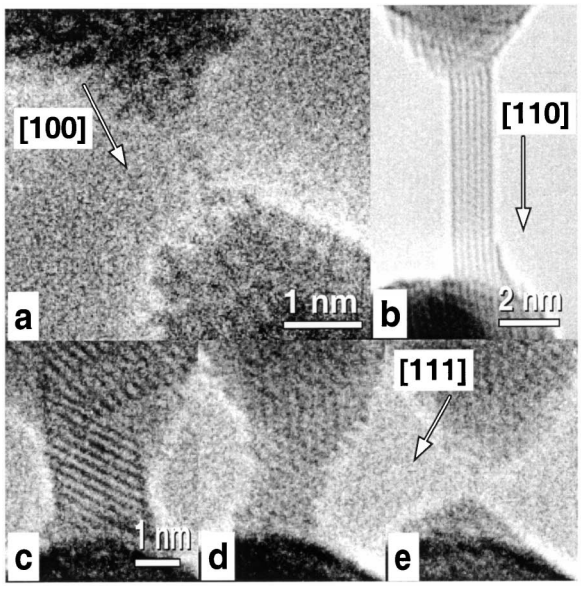

FIG. 2. HRTEM images of gold NWs; atomic positions appear dark. (a) [100] atom-chain NW; (b) rodlike [110] NW; (c)–(e) temporal evolution of a NW formed when the apexes are sliding: 0, 17:12, and 24:15 min, respectively.

[111] and [100] wires form bipyramidal constrictions. A [111] NW [Fig. 3(a)] would be composed of two pyramids faceted by alternating 3 (111) and 3 (100) facets, while for [100] NWs the pyramids are generated by four low energy (111) facets [Fig. 3(b)]. The pillar shape of [110] NWs is due to two families of low energy (111) planes that lie parallel to the wire axis and, consequently, bipyramidal short constrictions become energetically unfavored. Three probable minimal cross sections for [110] wires are proposed in the left part of Fig. 3(c). The one marked 8/6 corresponds to the [110] projection of an Au_{38} truncated cuboctahedron [23]; this pillar would be generated by the alternate stacking of atomic planes with 8 and 6 atoms [marked with different tones in Fig. 3(c)]. A side-view projection of the two smaller rods (aspect ratio 2.5) is also presented. It must be noted that the minimal cross section of [110] NWs seems to be always larger than the one-atom-thick contacts allowed by [111] or [100] orientations.

It is now tempting to associate the proposed atomic arrangements with transport properties. Several studies have predicted that for gold, a monovalent metal, one-atom-thick contacts should have a conductance close to a single quantum [1,10,14,17,24–27]. On this simple basis, [111] and [100] NWs are expected to display a $\sim 1G_0$ conductance plateau, but [110] wires should not.

To provide a deeper understanding of NW conductance, it is necessary to compare conductance measurements with the expected transport properties of the three different NW structures mentioned above. A quantitative way to do so could be based on the statistical analysis of the occurrence of each NW type. We must emphasize that due to the complexity of NW experiments, the analysis of average behaviors has already been extensively applied in this field [3,8,9,15]. To estimate the NW appearance rate, we must take into account that there is no control of the crystal orientation of the surfaces generating the NWs in most of the used setups [2–9]. Thus there is no reason to suppose that a particular orientation would be dominant and that the final NW structural type would be determined by the closest zone axis to the elongation direction, as indicated by our HRTEM results. Hence, the appearance rate of each NW type becomes proportional to the multiplicity of the zone axis, namely 4 for the [111], 3 for the [100], and 6 for the [110] direction, with a total number of 13 possibilities. Briefly, we would expect that 7/13 ([111] and [100] NWs) of the generated wires should show a conductance plateau at $1G_0$.

To measure the curve profile occurrence, we have acquired several series of 500 conductance curves and simply counted the number of curves displaying the last conductance step close to $1G_0$ (visual analysis). The vast majority of the curves could be easily classified, because they showed flat plateaus close to the integer multiples of G_0 (Fig. 4). Some curves displayed rather noisy but horizontal plateaus [Fig. 4(b)], which were classified by their mean value; small shoulders were neglected [arrowed in Fig. 4(a)]. The results of our analysis are shown in Table I, and they show a remarkable agreement with our model (7/13 or 54%). Also, an important fraction ($\sim 1/3$) of the remaining 6/13 of the curves, associated with rodlike NWs, show a final step at $2G_0$ [e.g., Fig. 4(c)], indicating that this conductance value should be the minimal observable conductance plateau of [110] NWs; nevertheless, this study does not allow one to get any information about the atomic structure.

It would also be very interesting to discriminate among the conductance curves displaying a $1G_0$ plateau, which ones are generated by the [100] or the [111] NWs. In a rather simple view, the neck cross-section variation must

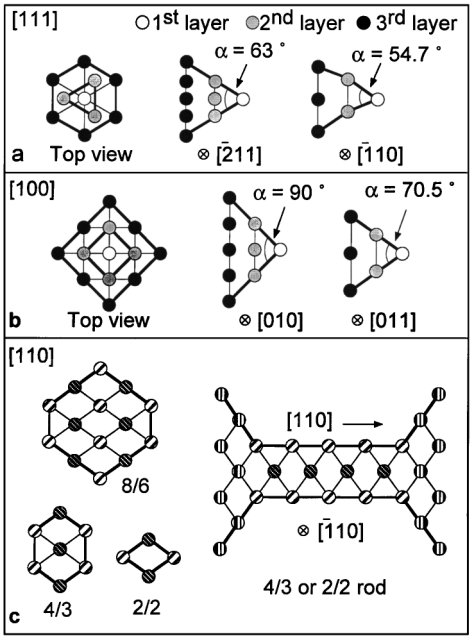

FIG. 3. Schema of possible atomic arrangement of gold NWs: (a) [111]; (b) [100]; (c) [110]. Top and side views are shown, also the observation axes and opening tip angles (α) are indicated. In (a) the tip atom sits at a hexagonal site. In (c) the left part shows the cross section of three possible [110] NWs, while a side view of the smaller rods is shown in the right part.

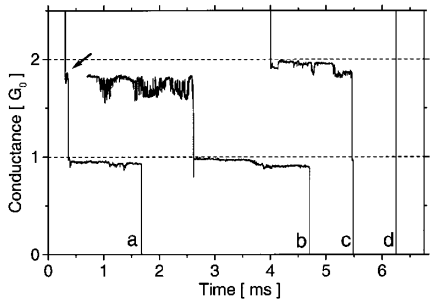

FIG. 4. Typical examples of gold NW conductance behaviors measured using the UHV-MCBJ. (*a*) single step at $\sim 1G_0$; (*b*) staircase profile with plateaus at $\sim 2G_0$ and $\sim 1G_0$; (*c*) last conductance plateau lying close to $2G_0$; (*d*) abrupt NW rupture.

TABLE I. Statistical analysis of conductance curves.

	Plateau at $1G_0$	Plateaus at $1G_0$ & $2G_0$
Expected values	54% (7/13)	31% (4/13)
Series 1	(52 ± 2)%	(34 ± 2)%
Series 2	(56 ± 2)%	(33 ± 2)%
Series 3	(50 ± 2)%	(31 ± 2)%

somewhat be related to the curve profile [2,8,11,13,27]. As [111] NWs display lower opening angles (see Fig. 3), they are the best candidates to display curves with steps at $1G_0$ and $2G_0$ (staircase profile, this definition neglects the conduction channel degeneracy [3] that has not been detected for gold [8,9,14,17,28,29]). The occurrence of conductance curves showing two plateaus, at $\sim 2G_0$ and $\sim 1G_0$, showed a remarkable agreement with the predicted value (4/13 or 31%) for [111] NWs (see Table I).

It must be remarked that the agreement with our model is obtained only when the gold surfaces are actually very clean. This is attained only during the first few hours after the initial wire fracture despite working in UHV [18]. Afterwards, some kind of contamination is evidenced by the additional plateaus at $\sim(0.1-0.2)G_0$ whose occurrence increases with the time. Then, the percentage related to the $1G_0$ plateau increases significantly ($\sim$65%–70%).

In summary, we have observed that just before rupture gold nanowires are crystalline and display only three possible atomic configurations where either [100], [110], or [111] directions lie approximately parallel to the elongation direction. Besides, NW mechanical behavior may be ductile or brittle, depending on the orientation. Using a simple crystallographic model, we have been able to estimate the NW atomic arrangement, conductance behavior, and occurrence probabilities. Comparisons with a typical experiment showed a remarkable agreement, indicating that it is possible to establish a correlation between the NW atomic arrangements and the conductance behavior for the final elongation steps. This statistical accordance corroborates the consistency of our model, providing a novel approach to analyze individual conductance curves instead of looking to average behavior [3,7–9]. This will stimulate more studies discriminating among structural and electronic effects and how they manifest in the conductance curve. This represents a fundamental issue to improve the understanding of several remaining open questions, such as deviations from perfect quantization [3,17,27,30] or valence band effects [24,25,27].

We thank CNPq and FAPESP (Contracts No. 1996/12546-0 and No. 1998/13501-6) for financial support. T. F. is grateful to the LNLS for funding. Professor W. A. de Heer is gratefully acknowledged for stimulating discussions.

*To whom correspondence should be addressed.
Email address: ugarte@lnls.br

[1] H. van Houten and C. Beenakker, Phys. Today **49**, No. 7 22 (1996).
[2] L. Olesen *et al.,* Phys. Rev. Lett. **72**, 2251 (1994).
[3] J. M. Krans *et al.,* Nature (London) **375**, 767 (1995).
[4] J. I. Pascual *et al.,* Science **267**, 1793 (1995).
[5] G. Rubio, N. Agraït, and S. Vieira, Phys. Rev. Lett. **76**, 2302 (1996).
[6] C. J. Muller, J. M. van Ruitenbeek, and L. J. de Jongh, Phys. Rev. Lett. **69**, 140 (1992).
[7] J. L. Costa-Krämer *et al.,* Surf. Sci. **342**, L1144 (1995).
[8] M. Brandbyge *et al.,* Phys. Rev. B **52**, 8499 (1995).
[9] K. Hansen *et al.,* Phys. Rev. B **56**, 2208 (1997).
[10] T. N. Todorov and A. P. Sutton, Phys. Rev. Lett. **70**, 2138 (1993).
[11] A. M. Bratkovsky, A. P. Sutton, and T. N. Todorov, Phys. Rev. B **52**, 5036 (1995).
[12] U. Landman *et al.,* Phys. Rev. Lett. **77**, 1362 (1996).
[13] M. R. Sørensen, M. Brandbyge, and K. W. Jacobsen, Phys. Rev. B **57**, 3283 (1998).
[14] H. Ohnishi, Y. Kondo, and K. Takayanagi, Nature (London) **395**, 780 (1998).
[15] A. I. Yanson *et al.,* Nature (London) **395**, 783 (1998).
[16] T. Kizuka, Phys. Rev. Lett. **81**, 4448 (1998); T. Kizuka *et al.,* Phys. Rev. B **55**, R7398 (1997).
[17] C. J. Muller *et al.,* Phys. Rev. B **53**, 1022 (1996).
[18] V. Rodrigues, Master thesis, Universidade Estadual de Campinas, 1999; V. Rodrigues and D. Ugarte, Rev. Sci. Instrum. (to be published).
[19] Y. Kondo and K. Takayanagi, Phys. Rev. Lett. **79**, 3455 (1997).
[20] D. Ugarte, Nature (London) **359**, 707 (1992).
[21] U. Landman *et al.,* Science **248**, 454 (1990).
[22] U. Durig, in *Nanowires,* edited by P. A. Serena and N. Garcia, NATO ASI Series (Kluwer, Dordrecht, 1997), Vol. 340, pp. 275–300.
[23] L. D. Marks, Rep. Prog. Phys. **57**, 603 (1994).
[24] C. Sirvent *et al.,* Phys. Rev. B **53**, 16 086 (1996).
[25] E. Scheer *et al.,* Nature (London) **394**, 154 (1998).
[26] H. Häkkinen, R. N. Barnett, and U. Landman, J. Phys. Chem. B **103**, 8814 (1999).
[27] A. Levy Yeyati, A. Martin-Rodero, and F. Flores, Phys. Rev. B **56**, 10 369 (1997).
[28] A. I. Yanson and J. M. van Ruitenbeek, Phys. Rev. Lett. **79**, 2157 (1997).
[29] J. M. van Ruitenbeek *et al.,* in *Nanowires* (Ref. [22]), Vol. 340, pp. 251–261.
[30] W. A. de Heer and D. Ugarte, in *Nanowires* (Ref. [22]), Vol. 340, pp. 227–236; W. A. de Heer, S. Frank, and D. Ugarte, Z. Phys. B **104**, 469 (1997).